Journal of Constructional Steel Research 150 (2018) 329–345

Contents lists available at ScienceDirect

Journal of Constructional Steel Research

A modified DEB procedure for estimating seismic demands of multi-mode-sensitive damage-control HSSF-EDBs

Ke Ke [a,*], Michael C.H. Yam [b,c], Lu Deng [a], Qingyang Zhao [a,b]

[a] Hunan Provincial Key Laboratory for Damage Diagnosis of Engineering Structures, Hunan University, Changsha, China
[b] Department of Building and Real Estate, The Hong Kong Polytechnic University, Hong Kong, China
[c] Chinese National Engineering Research Centre for Steel Construction (Hong Kong Branch), The Hong Kong Polytechnic University, Hong Kong, China

ARTICLE INFO

Article history:
Received 18 March 2018
Received in revised form 10 August 2018
Accepted 21 August 2018
Available online 5 September 2018

Keywords:
Steel moment-resisting frame
High-strength steel
Energy dissipation bay
Multi-mode
Energy demand indices
Nonlinear static procedure

ABSTRACT

The core objective of this research is to develop a modified dual-energy-demand-index-based (DEB) procedure for estimating the seismic demand of multi-mode-sensitive high-strength steel moment-resisting frames with energy dissipation bays (HSSF-EDBs) in the damage-control stage. To rationally quantify both the peak response demand and the cumulative response demand which are essential to characterise the damage-control behaviour of the system subjected to ground motions, the energy factor and cumulative ductility of modal single-degree-of-freedom (SDOF) systems are used as core demand indices, and the contributions of multi-modes are included in the proposed method. A stepwise procedure based on multi-mode nonlinear pushover analysis and inelastic spectral analysis of SDOF systems is developed. Based on the numerical models validated by test results, the proposed procedure is applied to prototype structures with a ground motion ensemble. The satisfactory agreement between the estimates by the proposed procedure and the results determined by nonlinear response history analysis (NL-RHA) under the ground motions indicates that the modified DEB procedure is a promising alternative for quantifying the seismic demands of tall HSSF-EDBs considering both peak response and cumulative effect, and the contribution of multi-modes can be reasonably estimated.

1. Introduction

A fundamental objective of conventional seismic design is to ensure the survival of a structure under earthquake ground motions for fulfilling the life-safety purpose. In this context, practical seismic design methodologies are generally governed by ductility-based philosophy that pursues sufficient inelastic deformation and stable plastic energy dissipation of a structure. To survive a moderate-to-strong earthquake attack, the members and connections of a conventional steel moment-resisting frame (MRF) are allowed to enter the inelastic stage in rapid succession. Notwithstanding the satisfactory ductility and stable energy dissipation capacity of conventional steel MRFs, recent seismic loss estimations show that unacceptable post-earthquake damages and residual deformations [1,2] induced by the inelastic actions of structural members may result in long-time occupancy suspension for repairing works. For structures experiencing severe damages, complete demolition and re-construction are unavoidable, which can lead to substantial economic loss. In order to enhance the seismic resilience [3,4] of steel MRFs, the idea of developing innovative steel MRFs showing improved damage evolution mode and encouraging post-earthquake performance is attracting interests from research communities.

Recently, the concept of "hybrid-steel-based" [5,6] or "dual-steel-based" [7–10] steel MRFs was found to be promising for improving the seismic performance of steel MRFs. In particular, appropriate combination of structural elements of relatively lower strength (e.g. low-yield-point steel or mild carbon steel) with high-strength steel (HSS) members can decouple the inherent interdependence between the stiffness and strength of a steel MRF. Therefore, when a hybrid-steel-based MRF or a dual-steel-based MRF is subjected to a seismic event, the damage-control behaviour [11–14] that restricts inelastic damages in preselected members or locations can be guaranteed in a wide deformation range, which is very desirable for improving the seismic performance of steel MRFs.

The great potential of extending the hybrid-steel-based or the dual-steel-based concept to seismic resistant steel MRFs has been supported by recent works. For instance, Charney and Atlayan [5] developed the hybrid steel MRF constructed by members with different steel grades, and the sound seismic performance with reduced residual deformations of the system was validated by a numerical investigation. Dubina et al. [7] proposed that the rational utilisation of HSS in steel MRFs will facilitate the exploitation of plastic energy dissipation in beams without significant damages accumulated in columns or connections. More

* Corresponding author.
E-mail address: keke@hnu.edu.cn (K. Ke).

https://doi.org/10.1016/j.jcsr.2018.08.024
0143-974X/

recently, Ke and Chen [14] proposed the concept of a dual-steel-based steel MRF, namely, high-strength steel MRF equipped with energy dissipation bays (HSSF-EDB). In particular, the system is composed of a main frame of HSS and sacrificial beams of mild carbon steel in the energy dissipation bays. Under earthquake loadings, the energy dissipation bays act as active dampers and provide plastic energy dissipation, while the HSS main frame can respond elastically in the expected deformation range. In this context, a damage-control stage will be formed in the nonlinear pushover curve of a HSSF-EDB structure. Later, Ke and Yam [15] proposed a direct-iterative design approach for conducting preliminary design of a HSSF-EDB system achieving damage-control behaviour under expected seismic excitations.

From the perspective of performance-based seismic engineering and seismic resilience enhancement, a methodology for prescribing the seismic demand of HSSF-EDBs in the damage-control stage where the HSS MRF generally stays elastic is a critical issue. In practical engineering, static evaluation procedures (e.g. nonlinear pushover analysis method), which enable designers to reasonably quantify the nonlinear seismic demand of a structure before it can be analysed with a more rigorous approach, i.e. the nonlinear response history analysis (NL-RHA), are generally preferred in the design procedure. In this respect, Ke et al. [16] recently developed the dual-energy-demand-index-based (DEB) procedure for quantifying the demand indices of low-to-medium-rise damage-control systems under expected earthquake ground motions. Specifically, based on single-degree-of-freedom (SDOF) systems with significant post-yielding stiffness ratio that can generally describe the nonlinear behaviour of a structure in the damage-control stage, the energy factors [15–20] deduced from the modified Housner principle [21] and the cumulative ductility [22–24] determined from the total dissipated plastic energy are used as the core demand indices to prescribe the seismic demand of a structure. As a typical evaluation procedure using multiple performance indices [25,26] for prescribing seismic demand, the DEB procedure prescribes the peak response demand and the cumulative response demand concurrently. Nevertheless, since only the fundamental vibration mode is considered in the DEB procedure, it is valid only for low-to-medium-rise structures. Therefore, for taller HSSF-EDBs which may show high sensitivity to higher vibration modes, the quantification of seismic demands characterising the damage-control behaviour is computationally consuming as the performance evaluation may be totally dependent on the NL-RHA.

The present work is a continuation of the DEB procedure and contributes towards a practical evaluation method for quantifying the seismic demands of multi-mode-sensitive HSSF-EDBs in the damage-control stage which have not been considered in the previous studies. Based on the multi-mode nonlinear pushover analysis and energy balance of equivalent modal SDOF systems representing the essential modes of a structure, a modified DEB procedure is developed, and the rationale of the modified DEB procedure is also clarified in detail. To demonstrate the procedure, the modified DEB procedure is applied to prototype HSSF-EDBs that are appreciably influenced by multi-modes, and the results determined by the modified DEB procedure are compared with those determined by the conventional DEB procedure and those from NL-RHA.

2. Development of the modified dual-energy-demand-index-based (DEB) procedure

2.1. Underlying assumptions

The modified DEB procedure is motivated by the energy balance of equivalent modal SDOF systems for characterising the response of a multi-mode-sensitive HSSF-EDB acting as a multi-degree-of-freedom (MDOF) system under earthquake ground motions. In particular, the underlying assumptions are listed as follows:

(1) The seismic energy balance of the entire structure as a MDOF system can be represented by the energy balance of the equivalent modal SDOF systems of essential modes, and the coupling effect among modal SDOF systems arising from the inelastic action of the structure is neglected.
(2) The superposition of the seismic responses of equivalent modal SDOF systems for characterising the behaviour of the entire MDOF system can be extended to inelastic stage for practical applications.
(3) The pushover response curve (skeleton response curve) of a HSSF-EDB can be approximated by a trilinear idealisation, and a bilinear kinematic model with significant post-yielding stiffness ratio can be utilised to describe the response curve of the system in the damage-control stage.

It is worth pointing out that although the utilisation of the first two assumptions compromises the theoretical rigorousness of preserving the computational simplicity of a static procedure, the rationale is in line with the widely used modal pushover analysis procedure [27], and the effectiveness of the two assumptions for practical applications is validated by extensive research works [28–30]. As for the third assumption, the viability has also been echoed by the test results extracted from the experimental programme of a large-scale HSSF-EDB [14,15]. The feasibility of using the multi-linear approximation for idealising the nonlinear pushover curve of a structure is supported by research findings from recent investigations [27–30] and documented in design specifications [31,32]. The accuracy of all these assumptions for quantifying the seismic demand of multi-mode-sensitive HSSF-EDBs in the damage-control stage will be further validated in the following sections.

2.2. Dual-energy-demand indices of equivalent modal SDOF systems

The fundamental performance requirements of HSSF-EDBs achieving the damage-control behaviour [16] are reproduced as follows: (1) The HSS MRF stays generally elastic under expected ground motions with damages locked in the energy dissipation bays equipped with sacrificial beams; (2) The sacrificial beams should provide a stable source of plastic energy dissipation to balance the accumulated plastic energy demand of earthquake ground motions. Thus, both the peak response demand and the cumulative response demand of a structure should be prescribed in seismic evaluations of the HSSF-EDBs.

A recent experimental investigation of a HSSF-EDB responding in the damage-control stage indicates that the nonlinear base shear versus displacement response can be idealised by a bilinear kinematic model with significant post-yielding stiffness ratio [15,16]. The good agreement between the test results and the idealised model curve is reproduced in Fig. 1a. Therefore, the bilinear kinematic hysteretic model with significant post-yielding stiffness ratio is assigned to the modal SDOF systems for developing the modified DEB procedure in this work. Accordingly, the seismic response of a tall HSSF-EDB can be simplified by the combination of the responses of equivalent modal SDOF systems representing essential modes. The energy factor (γ_n) of an equivalent modal SDOF system representing the "**n**th" mode is utilised to quantify the peak response demand considering the corresponding mode. As shown in Fig. 1b, the nominal absorbed energy defined by the covered area of the nonlinear base shear versus displacement curve of a SDOF system is calculated by the product of the energy factor and the absorbed energy of the corresponding elastic SDOF system assigned with the identical elastic properties (i.e. mass, stiffness and damping ratio) of the "**n**th" mode, and the energy balance equation for the SDOF system [15–17] is reproduced as follows:

$$\gamma_n E_{aen} = E_{an} \tag{1}$$

where E_{aen} = absorbed energy of the corresponding elastic SDOF

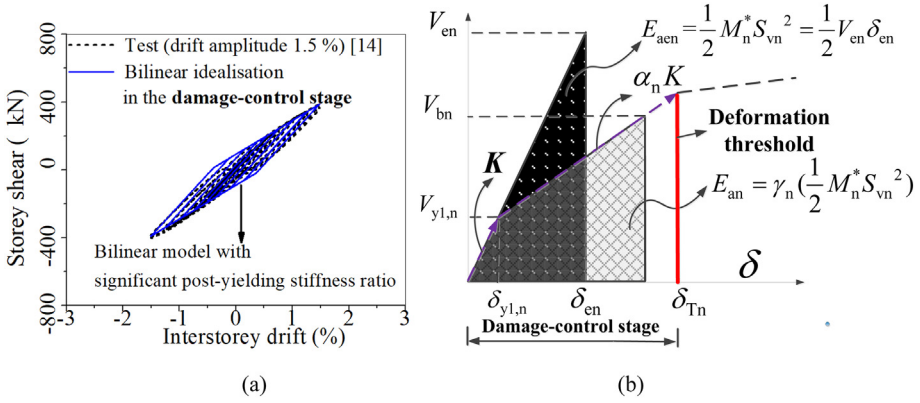

Fig. 1. Energy balance of multi-mode-sensitive HSSF-EDBs: (a) bilinear idealisation in the damage-control stage and the test result [14] and (b) energy balance of equivalent SDOF systems for the "nth" mode.

system for the "**n**th" mode and E_{an} = nominal absorbed energy of the inelastic SDOF system for the "**n**th" mode, as illustrated in Fig. 1b. Based on the nonlinear quantities characterising the hysteretic behaviour of the SDOF system, the energy factor of the "**n**th" mode is given as

$$\gamma_n = \frac{E_{an}}{\frac{1}{2}M_n^* S_{vn}^2} = \frac{\frac{1}{2}V_{y1,n}\delta_{y1,n} + (\zeta_n - 1)V_{y1,n}\delta_{y1,n} + \frac{1}{2}(\zeta_n - 1)^2\alpha_n V_{y1,n}\delta_{y1,n}}{\frac{1}{2}V_{en}\delta_{en}} = \chi_n(\alpha_n, \zeta_n, T_n, \xi_n)\left[2\zeta_n - 1 + \alpha_n(\zeta_n - 1)^2\right] \quad (2)$$

$$\zeta_n = \frac{\delta_n}{\delta_{y1,n}} \quad (3)$$

$$\chi_n = \left(\frac{V_{y1,n}}{V_{en}}\right)^2 \quad (4)$$

where $\delta_{y1,n}$ = first yield displacement corresponding to yielding of the energy dissipation bays for the "**n**th" mode; $V_{y1,n}$ = first yield base shear corresponding to yielding of the energy dissipation bays for the "**n**th" mode; δ_n = expected target displacement of the "**n**th" mode; α_n = post-yielding stiffness ratio of the nonlinear response curve in the damage-control stage for the "**n**th" mode; M_n^* = effective mass of the equivalent SDOF system for the "**n**th" mode [17]; δ_{en} = maximum displacement of the corresponding elastic SDOF system for the "**n**th" mode; V_{en} = maximum force of the corresponding elastic SDOF system for the "**n**th" mode; S_{vn} = spectral pseudo-velocity determined from an elastic spectral analysis of the SDOF system under a ground motion for the "**n**th" mode and χ_n = damage-control factor of the "**n**th" mode, which is dependent on the nonlinear quantities (α_n and ζ_n), the period (T_n) and the damping ratio (ξ_n) of the representative SDOF system. The definitions of the symbols are also indicated in Fig. 1b. It is worth pointing out that the energy factor of the SDOF system for the "**n**th" mode presented in Eq. (2)-Eq. (4) is applicable to the system responding in the damage-control stage, and the maximum displacement should not exceed the deformation threshold (i.e. $\delta_{Tn} = \zeta_{Tn}\delta_{y1,n}$) that represents the yielding point of the HSS MRF in the entire structure, as given in Fig. 1b. Hence, the following precondition should be satisfied.

$$\zeta_n \le \zeta_{Tn} \quad (5)$$

Note that the nonlinear base shear versus displacement response of the SDOF system for the "**n**th" mode and the essential quantities discussed above can be obtained by a nonlinear pushover analysis with the corresponding lateral force distributions on the numerical model of the entire structure, which will be further clarified in later sections.

For the cumulative ductility [23,24] quantifying the normalised accumulated energy demand of HSSF-EDBs in the damage-control stage, the index for the "**n**th" mode is given as follows:

$$\mu_{an} = \frac{E_{pn}(\alpha_n, \zeta_n, T_n, \xi_n)}{(1-\alpha_n)V_{y1,n}\delta_{y1,n}} \quad (6)$$

where E_{pn} = plastic energy dissipated by the equivalent SDOF system representing the "**n**th" mode. For structures responding in the damage-control stage, μ_{an} quantifies the cumulative energy demand of the sacrificial beams in the energy dissipation bays contributed by the "**n**th" mode.

2.3. A modified dual-energy-demand-index-based (DEB) damage-control evaluation procedure

In a previous work [16], the DEB procedure was proposed to prescribe the demand indices of low-to-medium-rise damage-control structures dominated by the fundamental vibration mode. Recognising that seismic responses of tall HSSF-EDB will be governed by multi-modes, a modified DEB procedure considering multi-modes is developed in this study for quantification of the seismic demand of the system in the damage-control stage. In general, the basic concept of the procedure is to use equivalent SDOF systems to characterise the seismic demand of tall HSSF-EDBs in the damage-control stage, and the effect of higher vibration modes is included. Accordingly, a step-by-step static evaluation procedure is established utilising the dual-energy-demand indices for all the essential modes of a HSSF-EDB, and it is presented as follows:

Step 1: Compute the elastic vibration properties of a HSSF-EDB structure considering the essential modes, i.e. the period T_n, the effective mass M_n^*, the modal vector $\boldsymbol{\varphi}_n$, and the participation factor Γ_n. It is proposed that the sum of effective masses of the considered modes should be larger than 90% of the seismic mass of the entire structure [32].

Step 2: Perform modal pushover analyses considering the essential modes. In particular, the invariant lateral load distributions used in various research works [27–30] are adopted, and the load distributions are reproduced as follows:

$$\mathbf{S}_n = \mathbf{m}\boldsymbol{\varphi}_n \quad (7)$$

where $\mathbf{S}_n$ = lateral load distribution vector of the "**n**th" mode; $\mathbf{m}$ = mass matrix; and $\boldsymbol{\varphi}_n$ = modal vector of the "**n**th" mode. Note that in this step, the P-Δ effect should be included by performing a static analysis with gravity load before pushover analysis.

Step 3: Utilising the data pool obtained by the pushover analyses in Step 2, the structure as a MDOF system is converted to the corresponding modal SDOF systems, and essential response curves of the

equivalent modal SDOF systems are developed. The concept of the energy-based SDOF system proposed by the previous work [16,33] is utilised, and the nominal energy capacity curves of each mode are developed with an incremental approach, as schematically illustrated in Fig. 2. In particular, accepting the first assumption in Section 2.1, the coupling effect among modal SDOF systems arising from the yielding of the structure can be neglected for practical applications, and thus the pushover loads of the "**n**th" mode only produce absorbed energy in the "**n**th" mode owing to the orthogonality of the vibration modes. In this context, the energy capacity curves are developed respectively considering the essential modes. More specifically, for the "**n**th" mode, based on the energy equilibrium principle that the external work done by the pushover lateral loads is identical to the absorbed energy of the system [16,17,33], the latter can be computed using the information about the lateral loads and the corresponding lateral displacements on each floor, as shown in Fig. 2a. Thus, the incremental absorbed energy can be determined by

$$\delta W_{\mathrm{n}}^{m}=\frac{1}{2}\left(\mathbf{S}_{\mathrm{n}}^{m-1}+\mathbf{S}_{\mathrm{n}}^{m}\right)\cdot\left(\mathbf{U}_{\mathrm{n}}^{m}-\mathbf{U}_{\mathrm{n}}^{m-1}\right) \tag{8}$$

where $\delta W_{\mathrm{n}}^{m}=$ incremental external work which is identical to the absorbed energy of the system at the "**m**th" step for the "**n**th" mode and $\mathbf{U}_{\mathrm{n}}=$ the lateral displacement vector corresponding to the

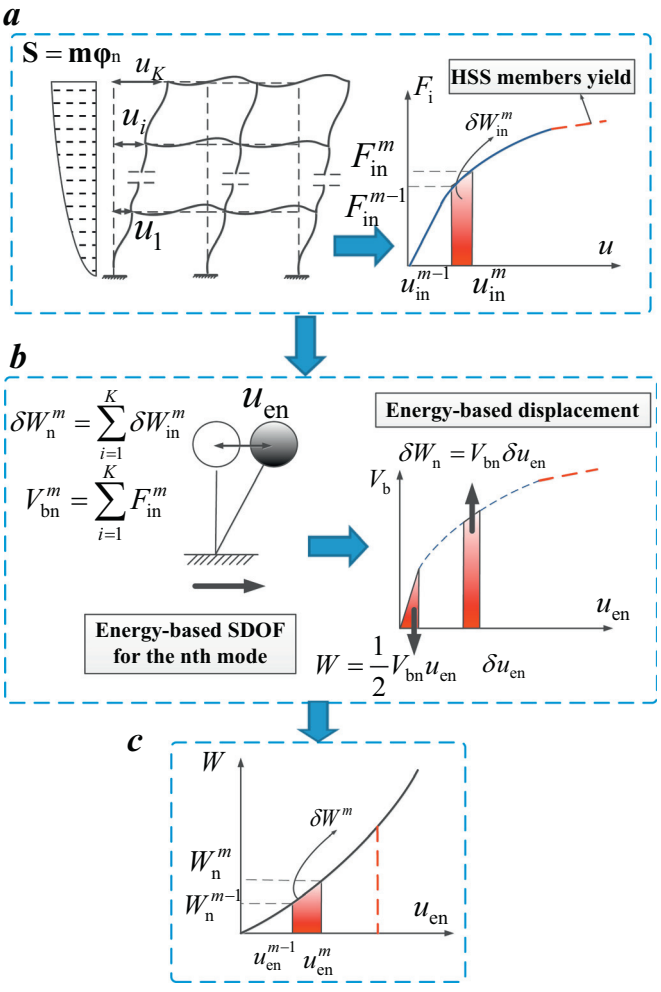

Fig. 2. Development of energy-based SDOF systems and the nominal energy capacity curves: (a) computation of absorbed energy under lateral loads, (b) development of energy-based SDOF systems and energy-based displacements and (c) construction of nominal energy capacity curves.

displacement profile of floors for a structure under the pushover load distribution of the "**n**th" mode.

Then, the energy-based displacement (u_{en}) of the SDOF system for the "**n**th" mode can be computed. As shown in Fig. 2b, when a system responds elastically, u_{en} can be directly determined based on the linear behaviour of the system. For both the elastic and the inelastic domain, the absorbed energy by the equivalent SDOF system for the "**n**th" mode in a differential displacement δu_{en} is equal to the work done by the lateral force distribution of the "**n**th" mode. In this context, the increment of the energy-based displacement at the "**m**th" step for the "**n**th" mode is reproduced and given by

$$\delta u_{\mathrm{en}}^{m}=\frac{\delta W_{\mathrm{n}}^{m}}{\frac{1}{2}\left(V_{\mathrm{bn}}^{m}+V_{\mathrm{bn}}^{m-1}\right)} \tag{9}$$

where $\boldsymbol{V}_{\mathrm{bn}}=$ the base shear of the equivalent SDOF system for the "**n**th" mode, which can be determined by the force equilibrium principle and given by

$$V_{\mathrm{bn}}^{m}=\mathbf{S}_{\mathrm{n}}^{m}\cdot\mathbf{1} \tag{10}$$

Therefore, the nominal energy capacity curve can be constructed (Fig. 2c), and the governing equations for developing the nominal energy capacity versus energy-based displacement curve for the energy-based SDOF system representing the "**n**th" mode are reproduced and given by

$$W_{\mathrm{n}}^{m}=W_{\mathrm{n}}^{m-1}+\delta W_{\mathrm{n}}^{m} \tag{11}$$

$$u_{\mathrm{en}}^{m}=u_{\mathrm{en}}^{m-1}+\delta u_{\mathrm{en}}^{m} \tag{12}$$

Step 4: Extract the base shear versus energy-based displacement curves from the response curves established in Step 3, and idealise the pushover curves (Fig. 2b) with a multi-linear approximation. In particular, a target displacement (u_{ent}) designated as the ultimate deformation should be defined first, as illustrated in Fig. 3a. In this respect, an approximate approach proposed by Ke and Chen [14] can be used. Then, the threshold representing the boundary of the damage-control stage for the "**n**th" mode can be identified (Fig. 3a). When the deformation is restricted below the threshold, the HSS frame will stay generally elastic.

Step 5: Based on the pushover responses till the displacement threshold defined in Step 4, use the bilinear idealisation documented in FEMA 273 [32] (Fig. 3b) to quantify the nonlinear parameters of pushover response in the damage-control stage, and the nonlinear quantities ($V_{\mathrm{y1,n}}$, α_{n}, ζ_{Tn}) of the equivalent energy-based SDOF system representing the "**n**th" mode can be confirmed.

Step 6: Develop the dual-energy-demand-index spectra for the essential modes following a constant-ductility method [15,16]. Note that various values of ζ_{n} should be employed as a basis for development of the demand curve in the next step.

Step 7: Develop the nominal energy demand curves for each mode utilising the energy factor spectra and the elastic spectral pseudo-velocity (S_{vn}) of ground motions, and the demand curve can be determined as follows:

$$E_{\mathrm{an}}=\gamma_{\mathrm{n}}(\alpha_{\mathrm{n}},\zeta_{\mathrm{n}},T_{\mathrm{n}},\xi_{\mathrm{n}})\frac{1}{2}M_{\mathrm{n}}^{*}S_{\mathrm{vn}}^{2} \tag{13}$$

Step 8: Plot the nominal energy capacity curve determined in Step 3 and the nominal energy demand curves obtained from Step 7 for each mode, and determine the peak response demand based on the intersection points of the demand curves and the capacity curves for the essential modes [16]. It is worth noting that the determined peak demand is valid when the intersection point of a demand curve (Step 7) and a capacity curve (Step 3) is captured in the damage-control stage for all the

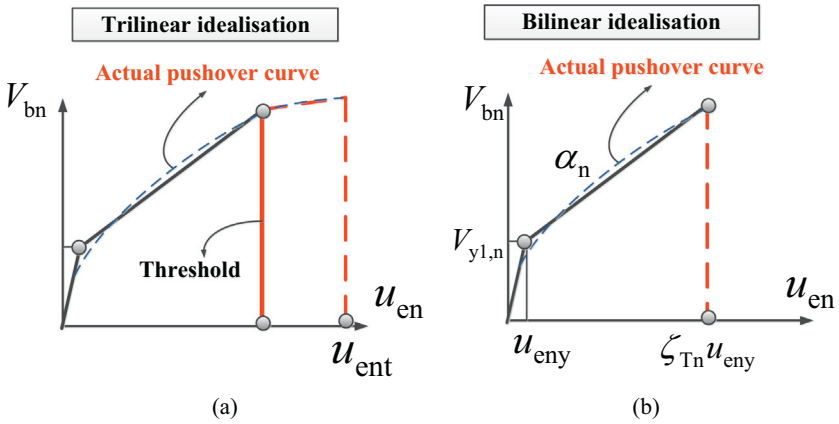

Fig. 3. Multi-linear idealisation of nonlinear responses: (a) trilinear idealisation and (b) bilinear idealisation.

essential modes. Otherwise, the HSS MRF in the structure is expected to experience evident inelastic deformation under the corresponding ground motions, and the bilinear model with significant post-yielding stiffness ratio is not applicable.

Step 9: For cases where the intersection points of the nominal energy demand curves and the corresponding energy capacity curves can be achieved for all the considered modes in the damage-control stage, the peak response demand of the energy-based SDOF systems of the "**n**th" mode under a ground motion is determined by the intersection point of the demand curve and the capacity curve of the corresponding mode. For the "**n**th" mode, extract the needed peak response quantities, e.g. roof displacement and interstorey drift, from the pushover database when the structure is pushed to the deformation corresponding to the intersection point, and the peak response of the MDOF system can be estimated using modal superposition following the second assumption stated in Section 2.1. For the HSSF-EDBs, the SSRS combination rule [27–30] is adopted, and the peak response is determined by

$$r_{MDOF} = \sum_{n=1}^{i} \left(r_n^2\right)^{0.5} \tag{14}$$

where r_{MDOF} = peak response of the entire structure and r_n = contribution of the "**n**th" mode.

Step 10: Compute the plastic energy of each mode (E_{pn}). For the "**n**th" mode, the intersection point extracted from Step 8 should be utilised to prescribe the corresponding ζ_n, and it can be substituted into Eq. (5). For simplicity, the total plastic energy dissipation of the structure is estimated by the summation of the dissipated plastic energy of the energy-based SDOF systems representing the essential modes, as given by

$$E_{p\text{-}all} = \sum_{n=1}^{i} E_{pn} \tag{15}$$

$$E_{pn} = u_{an} V_{y1,n} \delta_{y1,n} \tag{16}$$

where $E_{p\text{-}all}$ = estimated plastic energy dissipated by the entire structure. It is worth mentioning that the rationale of this step is supported by research works [34–36] on the correlation between the seismic energy response of a MDOF system and that of the corresponding modal SDOF systems.

Step 11: A modified energy profile method considering all the essential modes is developed based on the method proposed by Chou and Uang [34] is used to distribute the plastic energy over the structure. For the "**n**th" mode, it is assumed that the ratio of the plastic energy expected to be dissipated by the energy dissipation bay in a storey to the sum of the dissipated plastic energy in all storeys under ground motion is identical to that when the system is pushed to the peak deformation. Thus, in the damage-control stage, the plastic energy demand of the energy dissipation bay for the "**k**th" storey (K storeys in total), i.e. $E_{sp,k}$, considering the entire structure is determined as

$$E_{sp,k} = \sum_{n=1}^{i} \left(\frac{\eta_k}{\sum_{k=1}^{K} \eta_k} \right)_n E_{p,n} \tag{17}$$

where ηk = plastic energy dissipated by the energy dissipation bay of the "kth" storey when the structure is pushed to the target position where the energy-based displacement (uen) of the corresponding equivalent energy-based SDOF system reaches the intersection point determined by Step 8. A flowchart summarising the modified DEB procedure is presented in Fig. 4.

3. Demonstration of the procedure and discussions

3.1. Prototype structures and ground motions

To demonstrate the proposed modified DEB procedure and examine the effectiveness of the procedure for estimating the seismic demand of multi-mode-sensitive HSSF-EDBs in the damage-control stage, two tall prototype plane prototype structures are preliminarily designed according to a plastic design method proposed in [15] and the Chinese seismic provision, i.e. Chinese Code for Seismic Design of Buildings (GB 50011–2010) [37], and the basic acceleration is assumed to be 0.4 g. A dead load of 4.8 kN/m^2 and a live load of 2 kN/m^2 are assumed. The structural arrangement of the two systems is illustrated in Fig. 5a and Fig. 5b, respectively. In particular, for the 9-storey structure and the 12-storey structure, energy dissipation bays are equipped with mild carbon steel sacrificial beams with a yield stress of 235 MPa. To trigger the plastic energy dissipation of the sacrificial beams at relatively small drift level, reduced beams sections (RBSs) are considered in the sacrificial beams to further compromise the sectional yield moment capacity of the sacrificial beams. The RBS details satisfy the requirement of GB 50011–2010 [37] and AISC 358 [38], which are also provided in Fig. 5. The HSS frames are designed using HSS with a yield strength of 460 MPa and they are expected to stay elastic in a wider deformation range. Since the primary objective of the study is to examine the effectiveness of the modified DEB procedure for estimating the seismic demands of HSSF-EDBs in the damage-control stage, the two prototype structures are designed without considering structural optimisation.

To examine the accuracy of the developed procedure for quantifying the seismic demand quantities characterising the damage-control behaviour of HSSF-EDBs subjected to ground motions, twenty ground motions developed by Somerville et al. [39] (ground motion code: LA01-

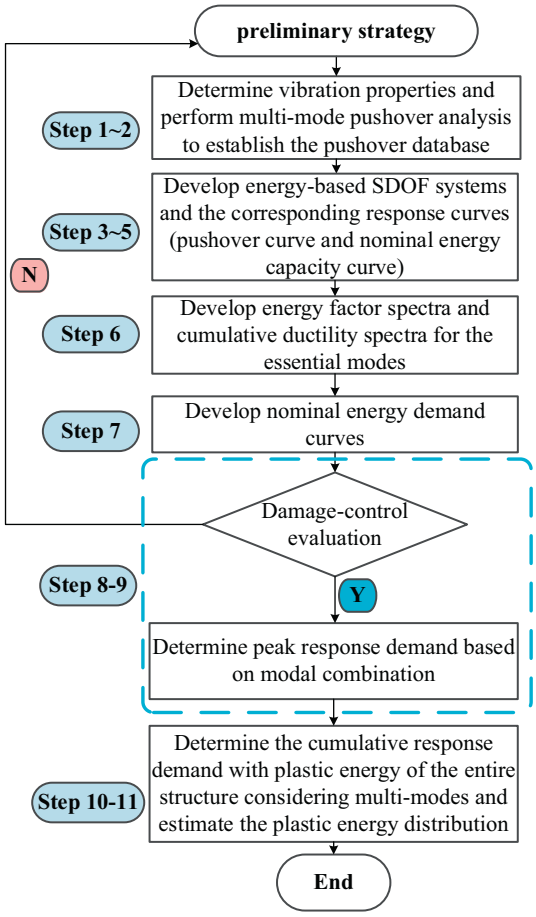

Fig. 4. Flowchart of the proposed modified DEB procedure.

LA20) for the SAC project are used in this study as excitations, and these records are for the hazard level with a probability of exceedance of 10% in 50 years considering the stiff soil.

3.2. Structural modelling strategy, validation and analysis types

In the present study, the commercial software ABAQUS [40] is utilised to develop the finite element (FE) models for the analysis. To validate the effectiveness of the modelling techniques for simulating the nonlinear behaviour of HSSF-EDBs, the test specimen of a HSSF-EDB from a large-scale experimental programme in [14] is modelled first, and the quasi-static test of the specimen is simulated by the analysis of the FE model. An overview of the FE model of the test specimen in [14] is provided in Fig. 6. In the FE model, to account for the potential influence of the asymmetric behaviour of the specimen, the twin frames are modelled. The two-node linear beam elements in space (shear-flexible 3-D beam elements with first order interpolation, i.e. B31 elements [40]) are used to simulate the columns and the beams in the specimen. For the sacrificial beams with RBSs in the energy dissipation bay, the mesh in the RBS region is refined, and the RBS segment was discretized by five B31 elements with varied flange widths, as shown in Fig. 6. For the prismatic members in the HSS MRF, uniform mesh is adopted. For simplification, all the joints are assumed rigid. The bilinear kinematic material model with von Mises criterion is utilised in the material model, and data input in the model is based on the true stress-strain curve extracted from the results of coupon tests. Note that the cyclic degradation of structural members and the fracture behaviour of the material are not considered in the modelling.

In the test, the ratio of the lateral load applied to the first floor to that on the second floor was 1:2 [14]. Thus, to replicate this lateral loading distribution, a rigid loading beam is introduced in the FE model, as shown in Fig. 6. In particular, the rigid beam placed at the midline of the specimen is connected with the twin frames on each floor with the "MPC pin" connectors [40], and the location of the load point in the model (point O in Fig. 6) can be determined according to the force equilibrium principle as follows:

$$FL = F_1 l_1 + F_2(l_2 + l_1) \tag{18}$$

$$F = F_1 + F_2 \tag{19}$$

$$2F_1 = F_2 \tag{20}$$

where F1 = load applied to the first floor; F2 = load applied to the second floor and F = load applied to the rigid loading beam. The other quantities in the equations discussed above are also indicated in Fig. 6. In the analysis, the vertical loads derived from the strain gauge readings are firstly applied to columns (Fig. 6), and the cyclic load is applied to the determined load point following the loading protocol of the test. The analysis is terminated at the load cycle corresponding to fracture inception in the test.

Fig. 7 presents the comparison of cyclic responses extracted from the analysis results and the counterparts from the test result database, and the moment (M) of representative members at a typical joint (Joint A in Fig. 6). The storey shear of the second storey (V_2) is plotted against the corresponding interstorey drift (θ_2). As can be seen, reasonable agreements between the predictions by the developed FE model and the test results are obtained.

Based on the above validated FE modelling techniques, the FE model of the prototype structures are developed. For the analysis works, both nonlinear static procedures (pushover analysis) and NL-RHAs are performed. In the analyses, P-Δ effects are considered by performing a static analysis considering the gravity load as the first step. The inertia forces in the NL-RHAs are considered by distributing the lumped mass on the corresponding floors. A damping ratio of 5% is considered for the first two modes to form the Rayleigh damping matrix.

3.3. Construction of equivalent energy-based SDOF systems

Frequency analyses are firstly performed to determine the vibration properties of the prototype structures, as given in Table 1. The mode shape component of the first three modes for the prototype structures is provided in Fig. 8.

Modal pushover analyses are performed using the lateral distributions given by Eq. (7) and the nonlinear response curves for the corresponding energy-based SDOF systems are developed (Step 3 in Section 2.3). As the first two modes of the prototype structures contribute to the total effective mass of over 90% of the total seismic mass, they are considered in the modal pushover analysis. For each mode, the two prototype structures are pushed to the state where the maximum interstorey drift (θ_{max}) reaches 2.5%, which can be recognised as the performance threshold for steel MRF structures [1,32,41], and the pushover responses of the energy-based SDOF systems characterising the nonlinear behaviour of the corresponding modes are given in Fig. 9.

The nonlinear behaviour of the energy-based SDOF systems is idealised by multi-linear approximations, and the corresponding threshold represented by the red dashed line quantifying the damage-control stage for each SDOF system is determined (i.e. ζ_{T1} and ζ_{T2} in Fig. 9). For cases where evident trilinear feature of the pushover responses (pushed to $\theta_{max} = 2.5\%$) is exhibited, the idealisation approach proposed by Ke and Chen [14] is utilised. Thus, the threshold is defined by the turning points representing the equivalent yield points of the HSS MRFs. For the cases in which a system stays in the damage-control stage, the bilinear estimation in FEMA-273 [32] is used to determine the approximate nonlinearity, and the threshold is prescribed by θ_{max} accordingly (Fig. 9d). It is worth noting that the prescription of threshold

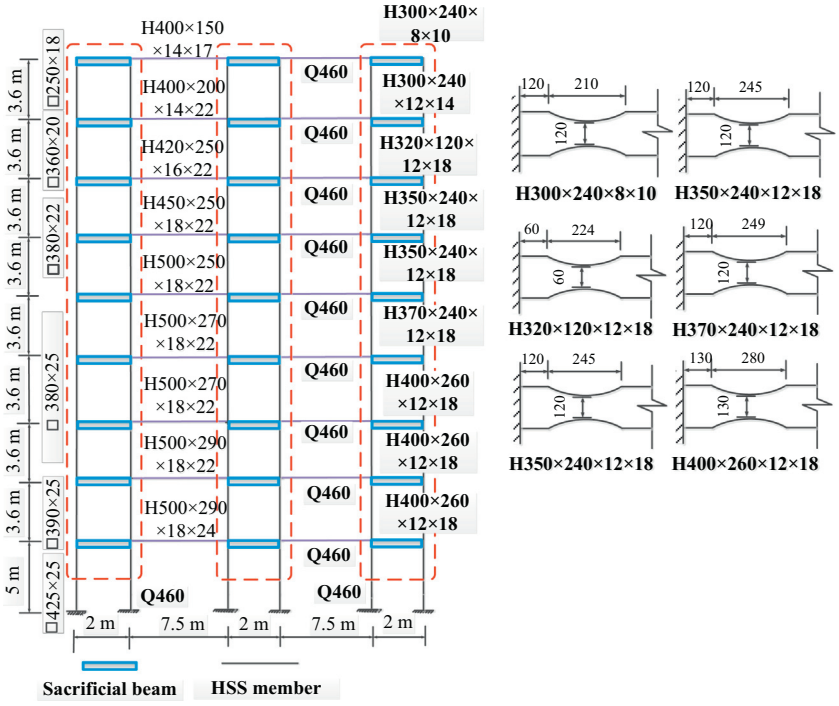

(a)

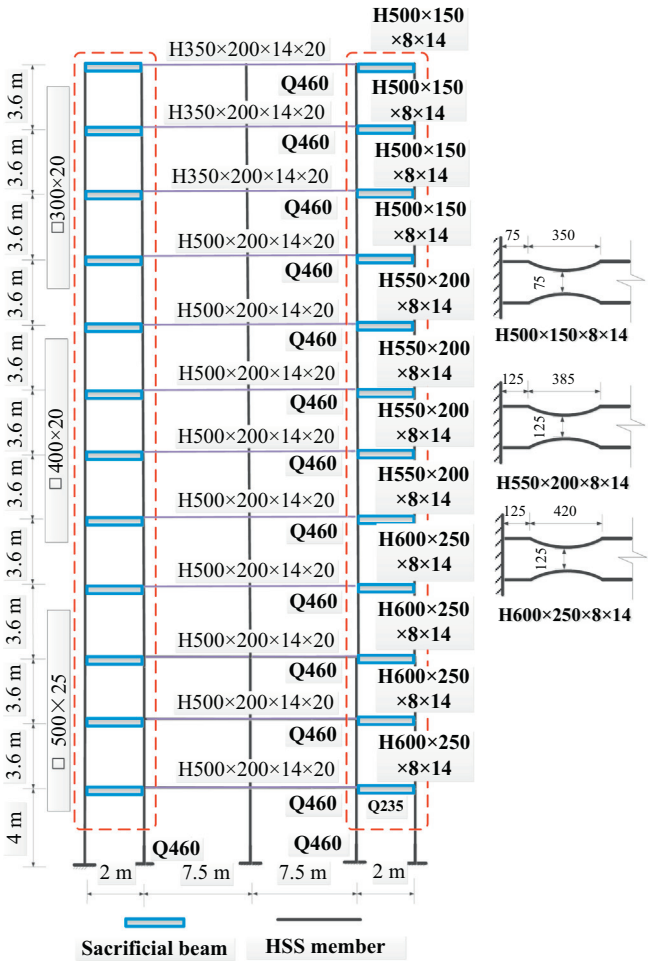

(b)

Fig. 5. Structural arrangement: (a) 9-storey structure and (b)12-storey structure.

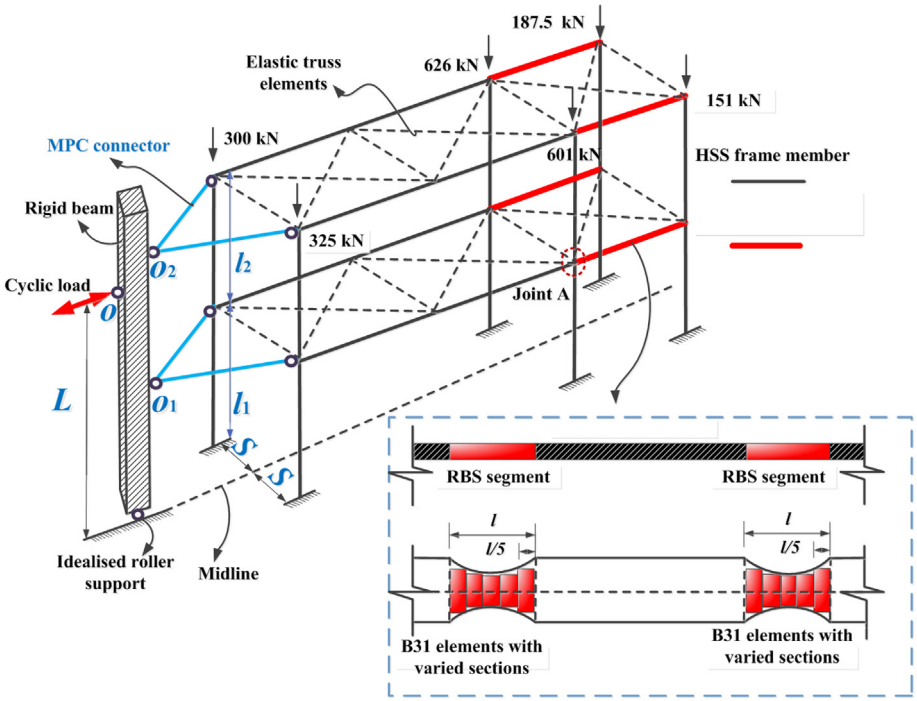

Fig. 6. Illustration of FE modelling of the test specimen in [14].

quantifying the threshold of the damage-control stage can also be adjusted flexibly. If the HSS MRF is expected to respond strictly damage-free, the threshold can be redefined based on the first yield point in the HSS frames [16], which can be extracted from the pushover database directly. However, as slight yielding behaviour of the HSS members does not lead to evident deterioration of the structural performance of

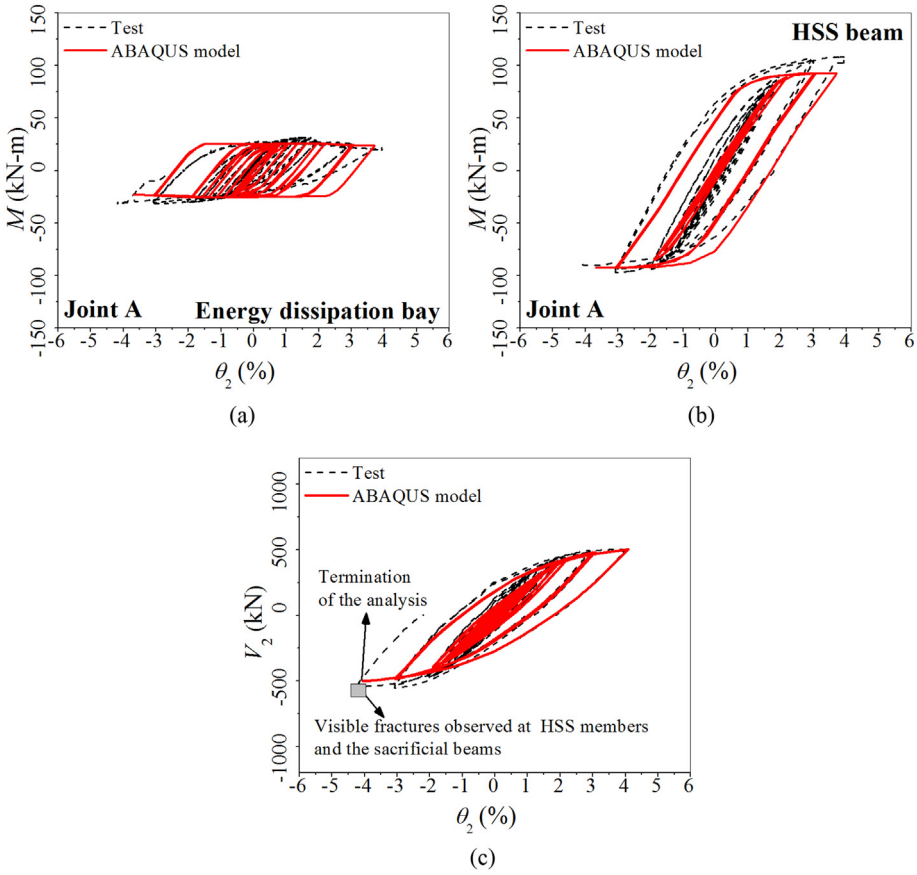

Fig. 7. Comparison of the FE results from the model and the test results from [14]: (a) moment of the sacrificial beam-interstorey drift response, (b) moment of the HSS beam-interstorey drift response and (c) storey shear- interstorey drift response.

Table 1
Information about the prototype structures.

Structure	Property (unit)	1st Mode	2nd. Mode	3rd mode
9-storey structure	Period (s)	1.56	0.55	0.32
	Modal effective mass (t)	673	99	31
	Modal participation factor	1.38	0.59	0.31
12-storey structure	Period (s)	2.35	0.82	0.44
	Modal effective mass (t)	797	171	60
	Modal participation factor	1.44	0.64	0.33

the frame, and the accuracy of the bilinear model with significant post-yielding stiffness ratio for quantifying the pushover response is quite satisfactory, as shown by Fig. 9, the procedure for determining the threshold based on the multi-linear approximation is viable in practice.

3.4. Development of dual-energy-demand-index spectra

The energy factor spectra are constructed utilising a constant-ductility method based on ground motion ensemble discussed in Section 3.1, and the data corresponding to the energy-based SDOF systems for the essential modes are presented in Fig. 10. The damping ratio is assumed to be 5% to maintain consistency, which is rational for steel structures. The energy factor was also used to quantify the seismic demand of ductile structures showing typical elastic-perfectly-plastic (EP) behaviour in recent research works [17–20], and a set of empirical equations based the classical Newmark and Hall inelastic spectra [43] were developed and extended to seismic design. Notwithstanding the computational attractiveness of the design equations, a recent study [16] has clarified the limitation of using energy factors of EP system for quantifying the seismic demand of damage-control structures with significant post-yielding stiffness ratio. Thus, to provide an in-depth understanding of the influence of hysteretic model on the energy factor, the energy factor spectra based on the Newmark and Hall spectra and the counterparts determined by a regression equation developed by Ke et al. [16] for systems in the damage-control stage with a damping ratio of 5% are also indicated in Fig. 10. As can be seen, good agreement between the mean energy factor spectra of the results from inelastic spectral analyses of the twenty ground motions and those by the regressed

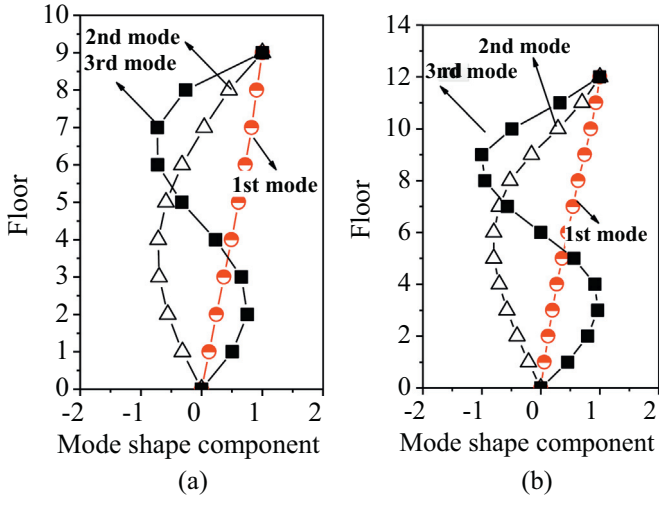

Fig. 8. Mode shape components of the modal vectors: (a) 9-storey structure and (b) 12-storey structure.

equation is observed, whereas evident non-conservative estimates are generated by those determined from the Newmark and Hall spectra for EP systems. It is worth pointing out that for tall HSSF-EDBs that are appreciably influenced by multi-modes, the inconsistent estimation of the energy factor would further compromise the accuracy in predicting the seismic demand of the entire structure, as errors might be accumulated for all the essential modes.

The cumulative ductility spectra for the energy-based SDOF systems are developed and presented in Fig. 11. The predictions by a set of equations proposed in [16] for prescribing the mean cumulative ductility demand for SDOF systems with significant post-yielding stiffness ratio are also indicated in the figure. In general, the cumulative ductility increases with increasing ζ_n for the first two modes of the prototype structures, implying that the cumulative effect would be pronounced if the damage-control stage of a pushover curve covers a wider deformation range after the yielding of sacrificial beams is activated.

3.5. Determination of peak response demand based on nominal energy demand curves and capacity curves

Based on the energy-based SDOF systems characterising the essential modes of the prototype structures, the nominal energy capacity curves are developed using the incremental approach given in Section 2.3. For the nominal energy demand curves, they are generated based on Eq. (13), and the demand index, i.e. energy factor, is extracted from the developed energy factor spectra discussed in Section 3.4. Then, the obtained demand curves and capacity curves are presented in the same diagram to perform the damage-control examination, and the data of energy-based displacement are normalised with ζ_n given by

$$\zeta_n = \frac{u_{en}}{u_{eyn}} \tag{21}$$

where ueyn = equivalent yield displacement of the energy-based SDOF systems for the "nth" mode (uey1 and uey2 in Fig. 9). The nominal demand curves and nominal capacity curves for the first two modes of the 9-storey prototype structure and the 12-storey prototype structure are presented in Fig. 12 and Fig. 13, respectively. The plastic energy dissipated by the HSS MRF from the results of NL-RHAs is also provided in Fig. 12c and Fig. 13c, respectively. It can be seen that the intersection points of the demand curves and the capacity curves can identify the damage state of HSS MRF with reasonable accuracy, as significant plastic energy dissipation of HSS MRF is obtained for cases in which the intersection points are above the defined threshold. It is worth mentioning that this threshold is determined by the equivalent yield point in the pushover responses as mentioned, and hence slight inelastic actions may have been triggered before the deformation reaching the equivalent point due to progressively yielding behaviour of the structure. Due to this reason, plastic energy dissipation of the HSS MRFs is observed in several cases where the intersection points are approaching the defined threshold, i.e. the 9-storey structure under LA14 ground motion (Fig. 12c) and the 12-storey structure under LA01, LA04 and LA11 ground motions (Fig. 13c). However, this negligible inelastic behaviour in HSS MRFs will not result in evident deterioration of the seismic resistance of the system. Also, engineers can adjust the threshold flexibly if more strict criteria for quantifying the performance of HSS MRFs should be applied.

For cases in which an intersection point can be obtained in the damage-control stage, the peak responses in terms of maximum roof displacement and maximum interstorey drift are obtained using Eq. (14) considering the first two modes. To illustrate the improved accuracy of the proposed modified DEB procedure for quantifying the peak response demand of HSSF-EDBs, the response quantities determined by the conventional DEB procedure that only accounts for the fundamental vibration mode are also obtained. In particular, the maximum roof displacement data determined by the modified DEB (MDEB) procedure

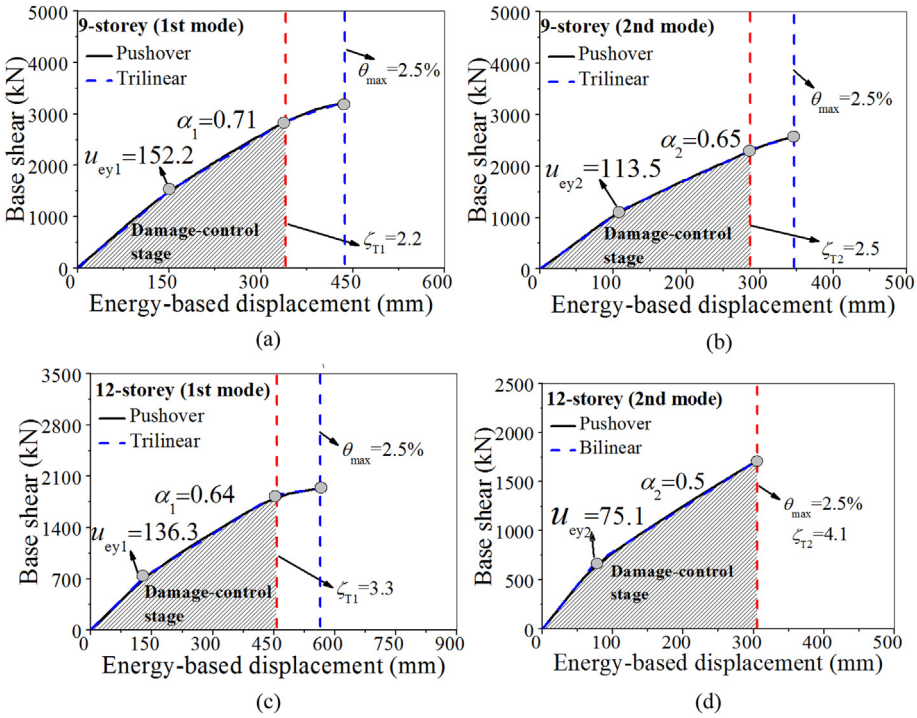

Fig. 9. Nonlinear responses of equivalent energy-based SDOF systems: (a) first mode of 9-storey structure, (b) second mode of 9-storey structure, (c) first mode of 12-storey structure, (d) second mode of 12-storey structure.

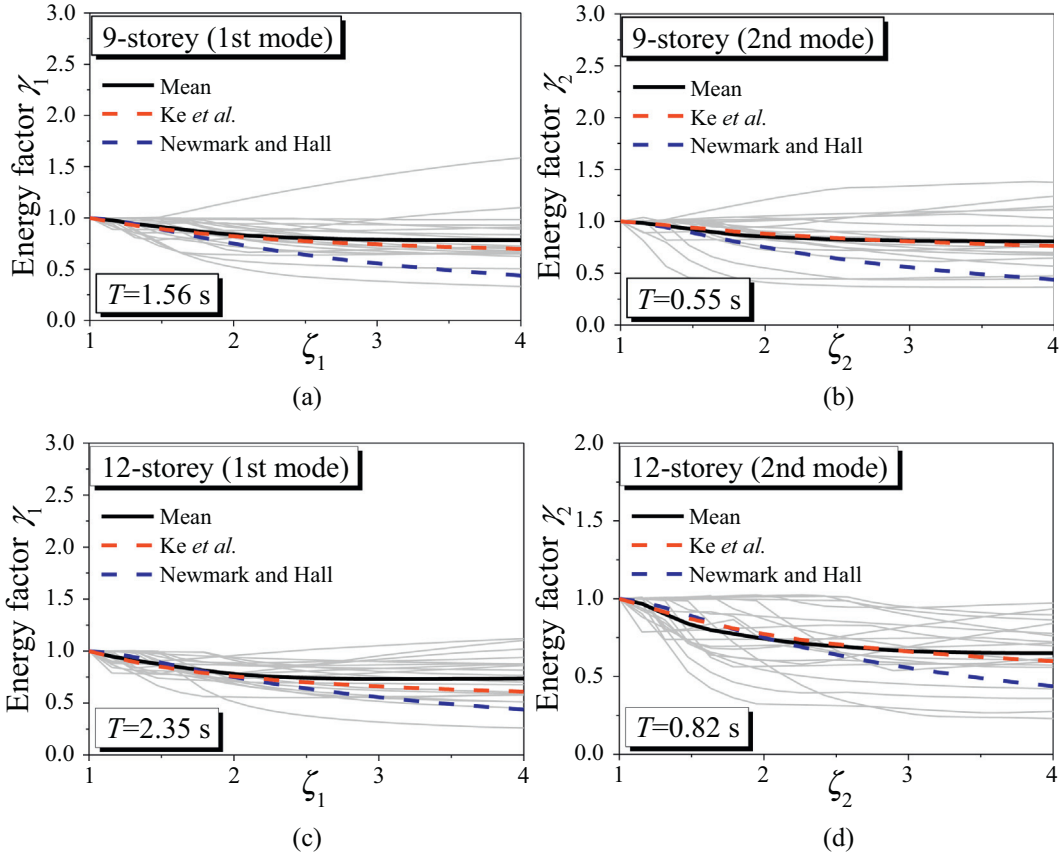

Fig. 10. Energy factor spectra of SDOF systems: (a) first mode of 9-storey structure, (b) second mode of 9-storey structure, (c) first mode of 12-storey structure, (d) second mode of 12-storey structure.

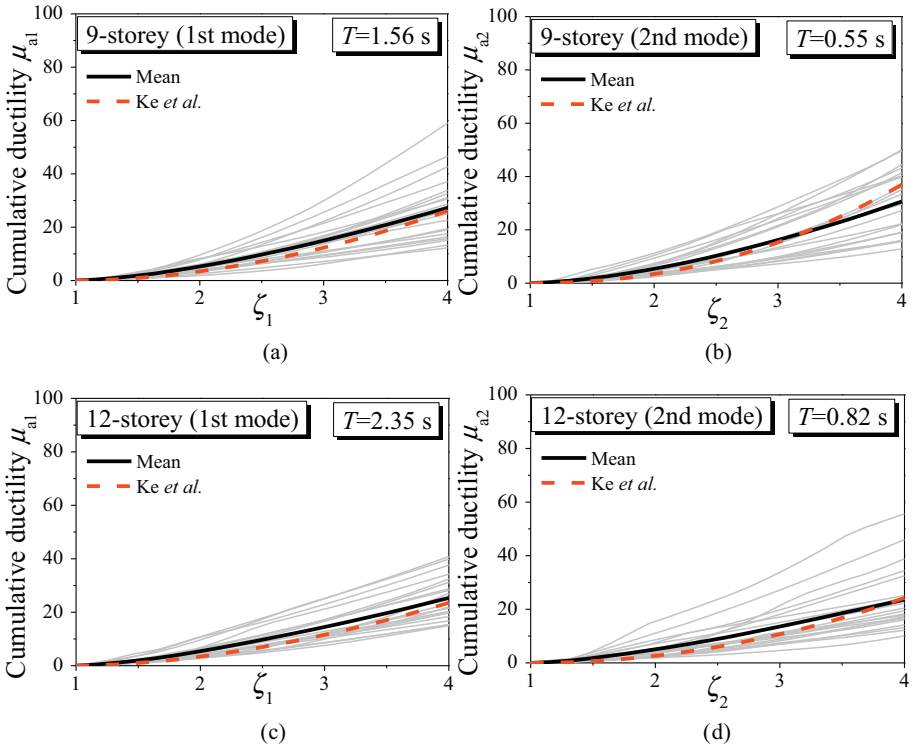

Fig. 11. Cumulative ductility spectra of SDOF systems: (a) first mode of 9-storey structure, (b) second mode of 9-storey structure, (c) first mode of 12-storey structure, (d) second mode of 12-storey structure.

(δ_{MDEB}) and those by the conventional DEB procedure (δ_{DEB}) are compared with the counterparts determined by the NL-RHAs ($\delta_{NL\text{-}RHA}$), as shown in Fig. 14a and b, respectively. For the prototype structures, the maximum roof displacement ratio ($\delta_{MDEB}/\delta_{NL\text{-}RHA}$ and $\delta_{DEB}/\delta_{NL\text{-}RHA}$) in average, denoted as Δ_{MDEB} and Δ_{DEB}, and the corresponding coefficient of variation (COV), denoted as ε_{MDEB} and ε_{DEB}, are also obtained and provided in the figure. For both the modified DEB procedure and the conventional DEB procedure, satisfactory predictions of the maximum roof displacement can be achieved as data points are clustered close to the forty-five degree diagonal line, and the modified DEB procedure results in relatively more conservative predictions as indicated by the average maximum roof displacement ratios.

Also, the maximum average interstorey drifts determined by the modified DEB procedures are extracted, and the predictions by the

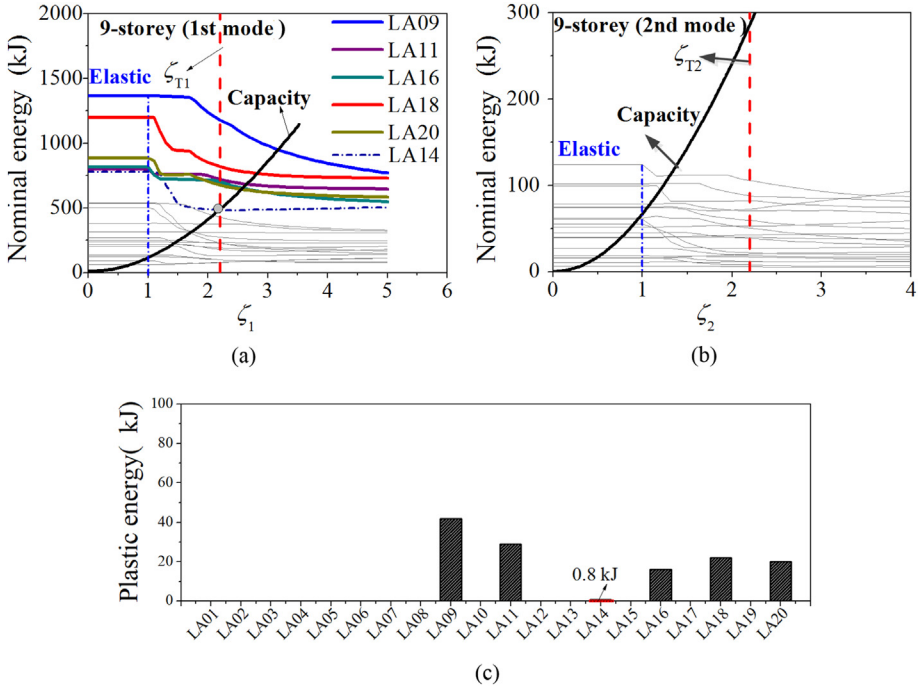

Fig. 12. Nominal energy demand, nominal energy capacity and plastic energy by NL-RHA of the 9-storey structure: (a) first mode, (b) second mode and (c) plastic energy in the HSS MRF under ground motions.

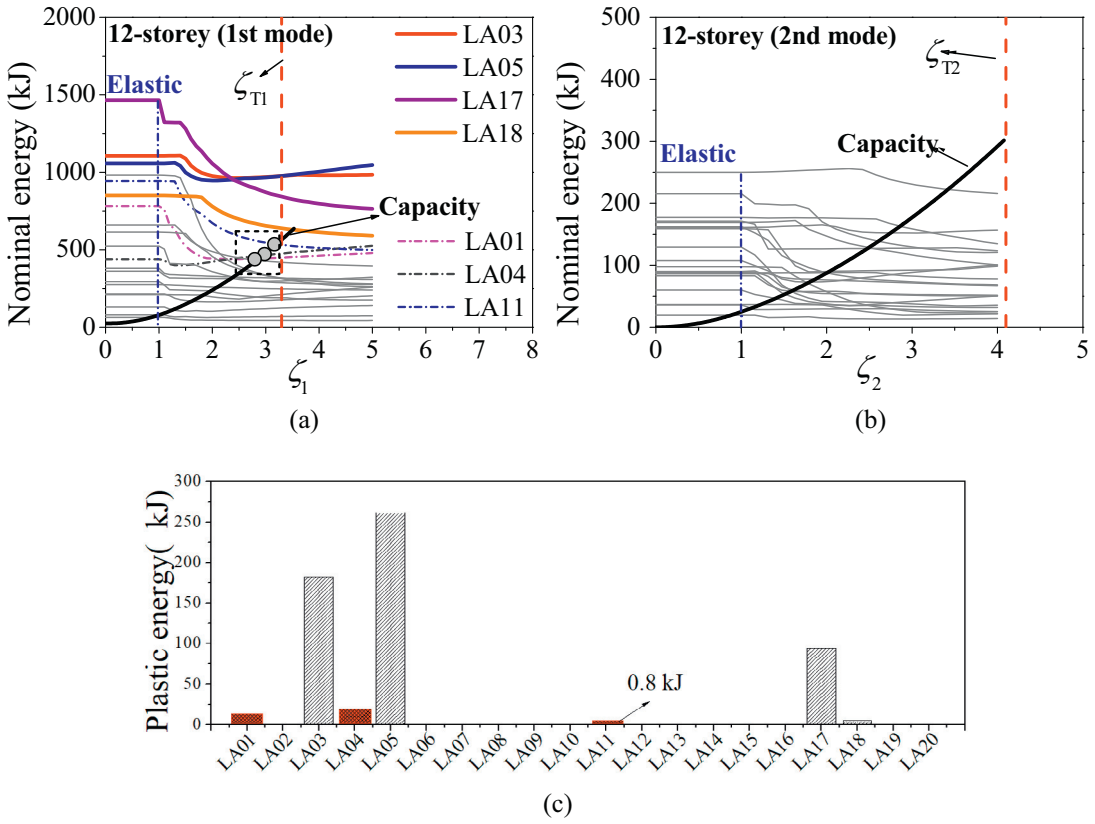

Fig. 13. Nominal energy demand, nominal energy capacity and plastic energy by NL-RHA of the 12-storey structure: (a) first mode, (b) second mode and (c) plastic energy in the HSS MRF under ground motions.

conventional DEB procedure accounting for the fundamental vibration mode are also obtained. To examine the effectiveness of the modified DEB procedure for predicting the peak interstorey drift demand, the responses by the two static procedures are compared with the counterparts determined by the NL-RHAs, as illustrated in Fig. 15. Compared with the conventional DEB procedure that significantly underestimates the peak interstorey drift, especially evident in upper floors, the proposed modified DEB procedure can produce reasonable estimates by accounting for the contribution of the higher mode that appreciably influence the seismic response of a tall HSSF-EDB in the damage-control stage.

To further examine the modified DEB procedure for predicting the peak response demand under an individual ground motion, the maximum interstorey drift responses determined by the modified DEB procedure (θ_{MDEB}), the conventional DEB procedure (θ_{DEB}) and the NL-RHA ($\theta_{NL\text{-}RHA}$) for each floor are extracted from the analysis database, and the corresponding maximum interstorey drift ratios for the "**i**th" storey are defined as follows:

$$(\lambda_{MDEB})_i = \left(\frac{\theta_{MDEB}}{\theta_{NL\text{-}RHA}}\right)_i \tag{22}$$

$$(\lambda_{DEB})_i = \left(\frac{\theta_{DEB}}{\theta_{NL\text{-}RHA}}\right)_i \tag{23}$$

The maximum interstorey drift ratios of the prototype structures are presented in Fig. 16. As can be seen, for both the 9-storey and 12-storey structures, the modified DEB procedure can lead to satisfactory

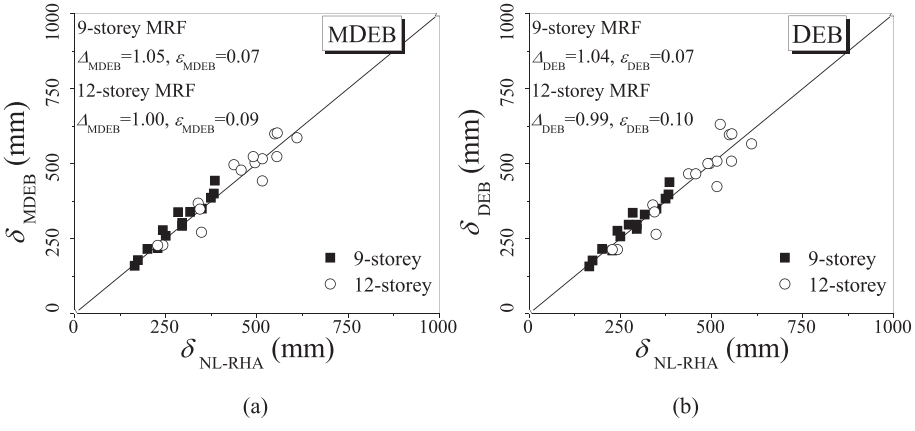

Fig. 14. Comparison of maximum roof displacement determined by static procedures with those from NL-RHAs: (a) modified DEB procedure and (b) DEB procedure.

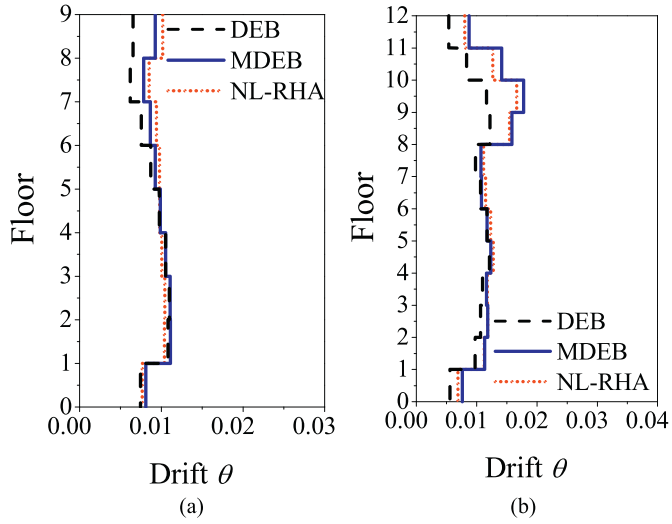

Fig. 15. Average interstorey drift responses determined by different procedures: (a) 9-storey structure and (b) 12-storey structure.

estimates of the maximum interstorey drift in general. In contrast, the conventional DEB procedure is inadequate to estimate the peak response demand by neglecting the contribution of higher modes, and the accuracy for predicting the peak interstorey drifts deteriorates significantly in the taller structure of which the higher mode is more influential.

3.6. Estimation of plastic energy distribution

The plastic energy of the entire structure can be evaluated for the essential modes based on the intersection points of the nominal energy demand curves and the corresponding capacity curves for each ground motion. The results are obtained according to the modified DEB procedure (E_{MDEB}) and the conventional DEB procedure (E_{DEB}) and they are compared with the counterparts determined by the NL-RHAs ($E_{NL\text{-}RHA}$) as shown in Fig. 17. The plastic energy ratios, i.e. $E_{MDEB}/E_{NL\text{-}RHA}$ and $E_{DEB}/E_{NL\text{-}RHA}$ on average, denoted as Δ^*_{MDEB} and Δ^*_{DEB}, are also produced in the figure along with the corresponding COVs, denoted as ε^*_{MDEB} and ε^*_{DEB}. As can be seen, the modified DEB procedure results in satisfactory predictions of the plastic energy demand, and the Δ^*_{MDEB} for both the 9-storey structure and the 12-storey structure is close to unity with a reasonable COV. In contrast, the conventional DEB procedure significantly underestimates the plastic energy demand of the prototype structures in many cases, particularly for the 12-storey

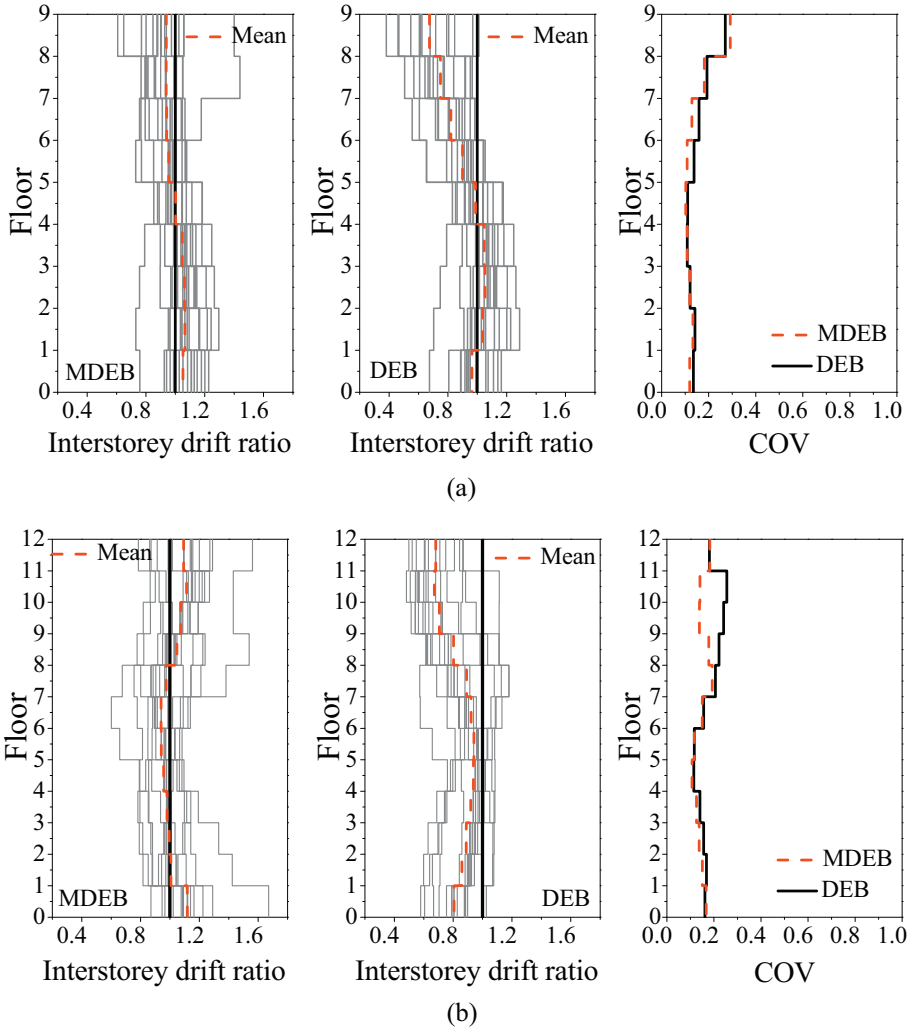

Fig. 16. interstorey drift ratios and the corresponding COVs by different static procedures: (a) 9-storey structure and (b) 12-storey structure.

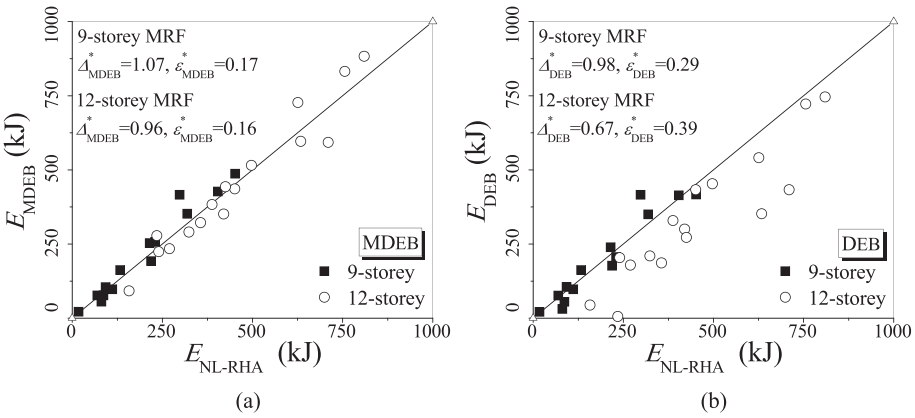

Fig. 17. Comparison of plastic energy dissipation demand determined by static procedures with those from NL-RHAs: (a) modified DEB procedure and (b) DEB procedure.

structure in which the higher vibration modes impose a more appreciable effect on the seismic demand of the system.

The plastic energy distribution of the prototype HSSF-EDBs subjected to ground motions determined by the refined energy profile method (see Section 2.3) is shown in Fig. 18. The results are compared with those obtained from the NL-RHAs. The plastic energy determined by the conventional DEB procedure are presented in the figure for comparison. For clarity, the responses are illustrated considering an individual ground motion.

3.7. Further discussion

The philosophy of the proposed procedure is in line with the existing static procedures, e.g. the modal pushover analysis [27–29] and the modified modal pushover analysis [44]. However, a critical issue of these analysis procedures is the accurate quantification of seismic demand indices. Notwithstanding the practical attractiveness of the widely used indices quantifying the strength demand [43,45–47] and the deformation demand [48–50] of the systems subject to ground motions, the current study is motivated by the energy balance concept. The necessity of using the dual-energy-demand indices for quantifying the seismic demand of a structure in the damage-control stage have been demonstrated by the previous work [16]. Specifically, it was observed that the peak response demand decreases with increasing inelastic deformation, whereas the reversed tendency of the cumulative response demand (i.e. plastic energy dissipation demand) was characterised. For tall HSSF-EDBs influenced by multi-modes, such inconsistent tendency would be amplified due to the modal combination, as can be seen from the energy factor spectra and the cumulative ductility spectra in Fig. 10 and Fig. 11, respectively. Thus, there is a high potential that the plastic energy demand can be tremendous even though the peak response demand is insignificant for a tall HSSF-EDB responding in the damage-control stage, and this study just puts forth a practical method to identify these extreme cases for achieving a safe design, and the limitation of the conventional DEB procedure is overcome.

Furthermore, when developing the multi-mode DEB procedure in the current study, a widely used assumption that the SDOF systems representing the higher modes stay elastic, which can facilitate the implementation of a static procedure [20,44], is not included. This is due to the fact that the yielding of sacrificial beams in the energy dissipation bays will be activated under lateral loads representing higher modes and produces plastic energy dissipation at low drift levels. Thus, for the HSSF-EDBs, assuming that higher modes stay elastic will result in non-conservative predictions for the plastic energy demand, although the peak responses would be overestimated, which can also be seen from the demonstration of the procedure discussed above. In particular, taking the 12-storey structure subjected to ground motion LA02 as an example, when using the modified DEB procedure to quantify the cumulative response demand, the estimated plastic energy contributed by the second mode reaches 41% to that by the sum of the first two modes, and hence the plastic energy dissipation distribution along the entire structure is appreciably influenced by the second mode (see Fig. 18b).

4. Conclusions

The present study proposes a modified DEB procedure for quantifying the seismic demand of multi-mode-sensitive high-strength steel (HSS) moment-resisting frames (MRFs) with energy dissipation bays (HSSF-EDB) in the damage-control stage. The proposed stepwise procedure motivated by the concept of equivalent energy-based SDOF systems is applied to prototype structures of tall HSSF-EDBs designed according to current seismic codes, and FE models of the prototype structures validated by a physical test programme are developed and analysed to illustrate the procedure. The effectiveness and the accuracy of the modified DEB procedure for quantifying the peak response demand and the cumulative response demand of the systems, which are both essential in performance-based seismic engineering, is examined by NL-RHA of the FE models. The improved accuracy of the procedure is also validated by comparing the determined results with those from the conventional DEB procedure which is rational for low-to-medium-rise structures whose performance is dominated by the fundamental vibration mode.

It is observed that for tall HSSF-EDBs in which multi-modes impose a significant effect on the seismic response of the system, the proposed modified DEB procedure that accounts for the contributions of higher modes can quantify the seismic demand of the system in the damage-control stage. In particular, by utilising the energy factor that characterises the peak response demand of equivalent energy-based SDOF systems, the maximum roof displacement and the maximum interstorey drifts response of the prototype tall HSSF-EDBs can be computed with satisfactory accuracy based on the SRSS modal combination rule by neglecting the coupling effect arising from the yielding of the system. Based on the peak response demand of equivalent SDOF systems representing the essential modes, the cumulative response demand of a structure in terms of plastic energy dissipation of the energy dissipation bays in each floor can also be quantified reasonably based on the proposed method. In contrast, the conventional DEB procedure considering the fundamental mode only produces reasonable estimates of roof displacement (drift), but produces inconsistent results of the maximum interstorey drift responses and plastic energy distributions along the structural height. Moreover, as the seismic demand of a tall HSSF-EDB is influenced by multi-modes, the reversed tendency of the peak response demand and cumulative response demand is more

evident. In this context, the proposed modified DEB procedure can be utilised to identify extreme cases where the cumulative energy demand is tremendous, whereas the peak response demand is insignificant.

It is worth pointing out that if the system experiences severe inelastic actions and the HSS members develop significant plastic deformations, the bilinear model with significant post-yielding stiffness ratio may result in biased estimates of the dual-energy-demand indices. Hence, a further study on extending the DEB procedure to quantify the seismic demand of multiple yielding stages of the HSSF-EDBs is being carried by the authors.

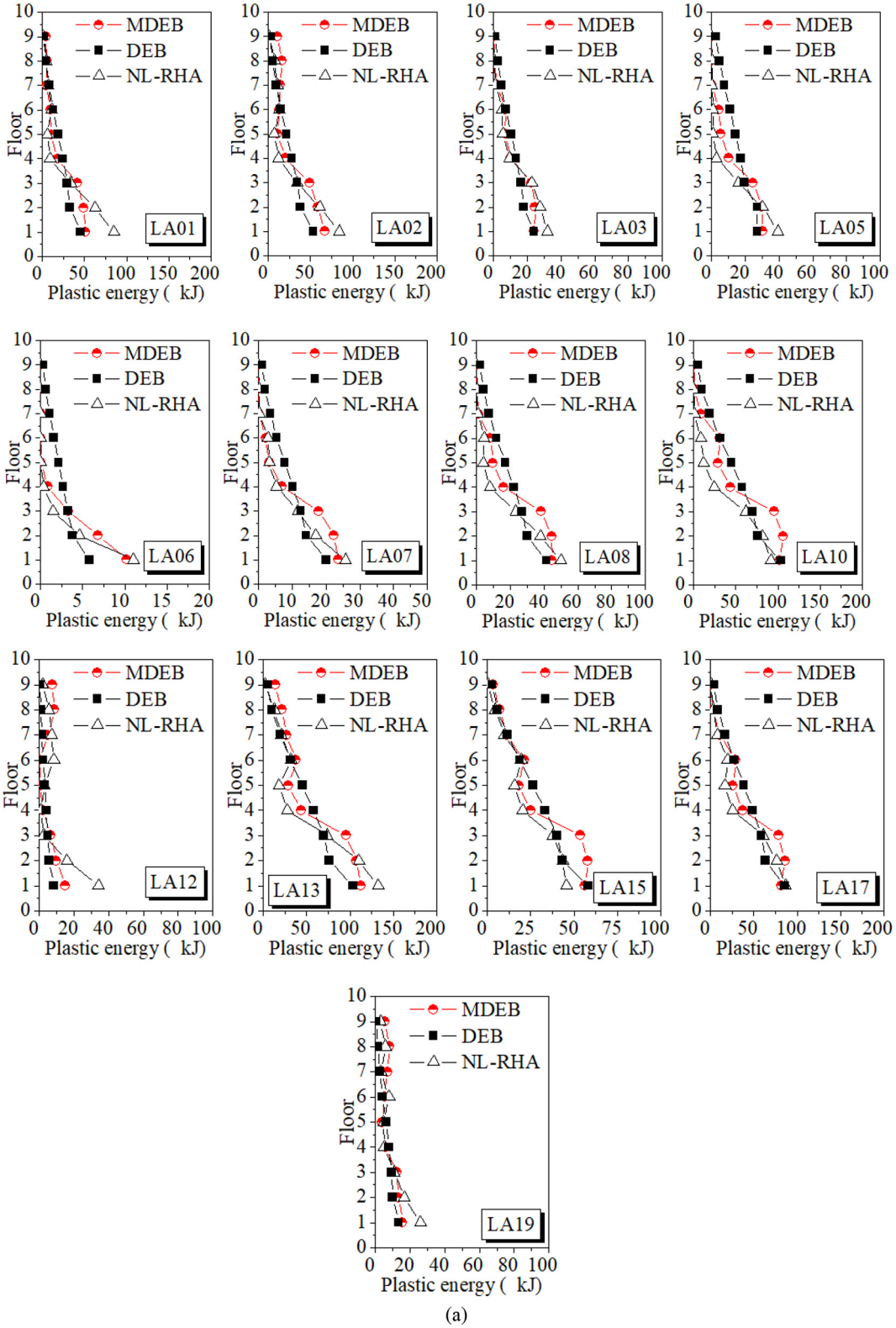

Fig. 18. Plastic energy dissipation determined by different procedures: (a) 9-storey structure and (b) 12-storey structure.

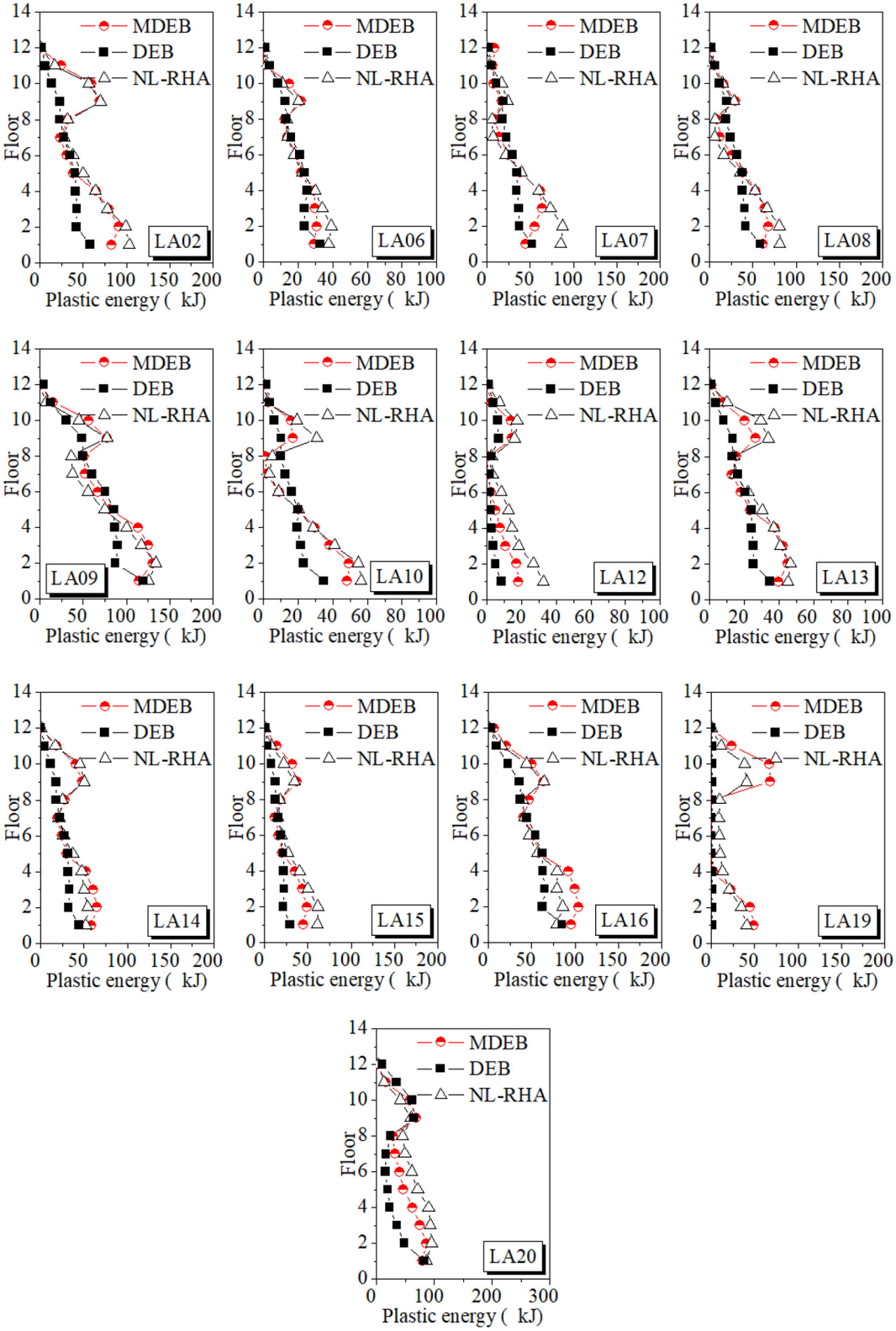

(b)

Fig. 18 (*continued*).

Acknowledgments

This research is financially supported by the National Natural Science Foundation of China (Grant No. 51708197) and the Fundamental Research Funds for the Central Universities of China (No. 531107050968). Partial funding supports provided by Chinese National Engineering Research Centre for Steel Connection, The Hong Kong Polytechnic University (Project No. 1-BBYQ) are also gratefully acknowledged.

References

[1] J. Erochko, C. Christopoulos, R. Tremblay, H. Choi, Residual drift response of SMRFs and BRB frames in steel buildings Designed according to ASCE 7-05, J. Struct. Eng. 137 (5) (2011) 589–599.
[2] D. Pettinga, C. Christopoulos, S. Parnpanin, et al., Effectiveness of simple approaches in mitigating residual deformations in buildings, Earthq. Eng. Struct. Dyn. 36 (12) (2007) 1763–1783.
[3] M. Bruneau, S.E. Chang, R.T. Eguchi, et al., A framework to quantitatively assess and enhance the seismic resilience of communities, Earthquake Spectra 19 (4) (2003) 733–752.
[4] G.P. Cimellaro, M.R.A.M. Bruneau, Framework for analytical qualification of disaster resilience, Eng. Struct. 32 (11) (2010) 3639–3649.
[5] F.A. Charney, O. Atlayan, Hybrid moment-resisting steel frames, Eng. J. AISC 48 (3) (2011) 169–182.
[6] O. Atlayan, F.A. Charney, Hybrid buckling-restrained braced frames, J. Constr. Steel Res. 96 (2014) 95–105.
[7] D. Dubina, F. Dinu, R. Zaharia, V. Ungureanu, D. Grecea, Opportunity and effectiveness of using high-strength steel in seismic resistant building frames, International Conference in Metal Structures, 2006.
[8] D. Dubina, A. Stratan, F. Dinu, Dual high strength steel eccentrically braced frames with removable links, Earthq. Eng. Struct. Dyn. 37 (15) (2008) 1703–1720.
[9] A. Tenchini, M. D'Aniello, C. Rebelo, R. Landolfo, L.S. Da Silva, L. Lima, Seismic performance of dual-steel moment resisting frames, J. Constr. Steel Res. 101 (2014) 437–454.
[10] A. Tenchini, M. D'Aniello, C. Rebelo, R. Landolfo, L.S. da Silva, L. Lima, High strength steel in chevron concentrically braced frames designed according to Eurocode 8, Eng. Struct. 124 (2016) 167–185.
[11] F. Ozaki, Y. Kawai, R. Kanno, K. Hanya, Damage-control systems using replaceable energy-dissipating steel fuses for cold-formed steel structures: seismic behaviour by shake table tests, J. Struct. Eng. 139 (5) (2012) 787–795.
[12] J.J. Connor, A. Wada, M. Iwata, Y. Huang, Damage-controlled structures. I: preliminary design methodology for seismically active regions, J. Struct. Eng. 123 (4) (1997) 423–431.
[13] R. Vargas, M. Bruneau, Experimental response of buildings designed with metallic structural fuses. II, J. Struct. Eng. 135 (4) (2009) 394–403.
[14] K. Ke, Y. Chen, Seismic performance of MRFs with high strength steel main frames and EDBs, J. Constr. Steel Res. 126 (2016) 214–228.
[15] K. Ke, M.C.H. Yam, A performance-based damage-control design procedure of hybrid steel MRFs with EDBs, J. Constr. Steel Res. 143 (2018) 46–61.
[16] K. Ke, M.C.H. Yam, S. Ke, A dual-energy-demand-indices-based evaluation procedure of damage-control frame structures with energy dissipation fuses, Soil Dyn. Earthq. Eng. 95 (2017) 61–82.
[17] S. Leelataviwat, W. Saewon, S.C. Goel, Application of energy balance concept in seismic evaluation of structures, J. Struct. Eng. 135 (2) (2009) 113–121.
[18] C. Zhai, D. Ji, W. Wen, W. Lei, L. Xie, Constant ductility energy factors for the near-fault pulse-like ground motions, J. Earthq. Eng. (2016) 1–16.
[19] D.R. Sahoo, S. Chao, Performance-based plastic design method for buckling-restrained braced frames, Eng. Struct. 32 (9) (2010) 2950–2958.
[20] Y. Jiang, G. Li, D. Yang, A modified approach of energy balance concept based multimode pushover analysis to estimate seismic demands for buildings, Eng. Struct. 32 (5) (2010) 1272–1283.
[21] G.W. Housner, Limit design of structures to resist earthquakes, Proceedings of the First World Conference on Earthquake Engineering, 1959.
[22] A. Surahman, Earthquake-resistant structural design through energy demand and capacity, Earthq. Eng. Struct. Dyn. 36 (14) (2007) 2099–2117.
[23] A. Teran-Gilmore, R. Simon-Velazquez, Use of cumulative ductility spectra within a deformation-control format for seismic design of ductile structures subjected to long duration motions, J. Earthq. Eng. 12 (1) (2008) 136–151.
[24] A. Teran-Gilmore, N. Bahena-Arredondo, Cumulative ductility spectra for seismic design of ductile structures subjected to long duration motions: Concept and theoretical background, J. Earthq. Eng. 12 (1) (2008) 152–172.
[25] J.W.W. Guo, C. Christopoulos, Performance spectra based method for the seismic design of structures equipped with passive supplemental damping systems, Earthq. Eng. Struct. Dyn. 42 (6) (2013) 935–952.
[26] J.W.W. Guo, C. Christopoulos, A procedure for generating performance spectra for structures equipped with passive supplemental dampers, Earthq. Eng. Struct. Dyn. 42 (9) (2013) 1321–1338.
[27] A.K. Chopra, R.K. Goel, A modal pushover analysis procedure for estimating seismic demands for buildings, Earthq. Eng. Struct. Dyn. 31 (3) (2002) 561–582.
[28] C. Chintanapakdee, A.K. Chopra, Evaluation of modal pushover analysis using generic frames, Earthq. Eng. Struct. Dyn. 32 (3) (2003) 417–442.
[29] H. Bobadilla, A.K. Chopra, Evaluation of the MPA procedure for estimating seismic demands: RC-SMRF buildings, Earthquake Spectra 24 (4) (2008) 827–845.
[30] A.H. Nguyen, C. Chintanapakdee, T. Hayashikawa, Assessment of current nonlinear static procedures for seismic evaluation of BRBF buildings, J. Constr. Steel Res. 66 (8–9) (2010) 1118–1127.
[31] CEN, EuroCode 8: Design Provisions for Earthquake Resistance-Part 1: General Rules, Seismic Actions and Rules for Buildings, European Committee for Standardization, Brussels, 2004.
[32] Federal Emergency Management Agency. NEHERP Provisions for the Rehabilitation of Buildings. FEMA No.273 (Guidelines) and 274 (Commentary), Washington, DC, 1997.
[33] E. Hernandez-Montes, O.S. Kwon, M.A. Aschheim, An energy-based formulation for first- and multiple-mode nonlinear static (pushover) analyses, J. Earthq. Eng. 8 (1) (2004) 69–88.
[34] C.C. Chou, C.M. Uang, A procedure for evaluating seismic energy demand of framed structures, Earthq. Eng. Struct. Dyn. 32 (2) (2003) 229–244.
[35] E. Kalkan, S.K. Kunnath, Effective cyclic energy as a measure of seismic demand, J. Earthq. Eng. 11 (5) (2007) 725–751.
[36] A. Habibi, R.W.K. Chan, F. Albermani, Energy-based design method for seismic retrofitting with passive energy dissipation systems, Eng. Struct. 46 (2013) 77–86.
[37] CMC, Code for Seismic Design of Buildings (GB 50011-2010), China Ministry of Construction, Beijing, 2010.
[38] AISC, Prequalified Connections for Special and Intermediate Steel Moment Frames for Seismic Applications, ANSI/AISC 358-10, American Institute for Steel Construction, Chicago, IL, 2010.
[39] P. Somerville, Development of Ground Motion Time Histories for Phase 2 of the FEMA/SAC Steel Project, SAC Background Document SAC/BD-91/04, SAC Joint Venture, Sacramento, Calif, 1997.
[40] ABAQUS Analysis User's Manual. ABAQUS Standard, Version 6.122012.
[41] FEMA, Pre-standard and commentary for the seismic rehabilitation of buildings, report FEMA-356, SAC Joint Venture for the Federal Emergency Management Agency, Washington, DC, 2000.
[43] N.M. Newmark, W.J. Hall, Earthquake Spectra and Design, Monograph, Earthquake Engineering Research Institute (EERI), Oakland (CA), 1982.
[44] A.K. Chopra, R.K. Goel, C. Chintanapakdee, Evaluation of a modified MPA procedure assuming higher modes as elastic to estimate seismic demands, Earthquake Spectra 20 (3) (2004) 757–778.
[45] K.T. Farrow, Y.C. Kurama, SDOF demand index relationships for performance-based seismic design, Earthquake Spectra 19 (4) (2003) 799–838.
[46] R.S. Jalali, M.D. Trifunac, A note on strength reduction factors for design of structures near earthquake faults, Soil Dyn. Earthq. Eng. 28 (3) (2008) 212–222.
[47] E. Miranda, Site-dependent strength reduction factors, J. Struct. Eng. ASCE 119 (12) (1993) 3503–3519.
[48] G.D. Hatzigeorgiou, D.E. Beskos, Inelastic displacement ratios for SDOF structures subjected to repeated earthquakes, Eng. Struct. 31 (11) (2009) 2744–2755.
[49] G.D. Hatzigeorgiou, G.A. Papagiannopoulos, D.E. Beskos, Evaluation of maximum seismic displacements of SDOF systems from their residual deformation, Eng. Struct. 33 (12) (2011) 3422–3431.
[50] A.K. Chopra, C. Chintanapakdee, Inelastic deformation ratios for design and evaluation of structures: Single-degree-of-freedom bilinear systems, J. Struct. Eng. ASCE 130 (9) (2004) 1309–1319.